

# Reactivity of Electron-Deficient Benzoheterocycle Triosmium Clusters. 5. The Chemistry of $\text{Os}_3(\text{CO})_9(\mu_3\text{-}\eta^2\text{-(C(9)-N)-5,6\text{-benzoquinoly}})(\mu\text{-H})$ and Its Phosphine Derivative<sup>‡</sup>

Ryan Smith and Edward Rosenberg\*

Department of Chemistry, The University of Montana, Missoula, Montana 59812

Kenneth I. Hardcastle, Venessa Vazquez, and Jay Roh

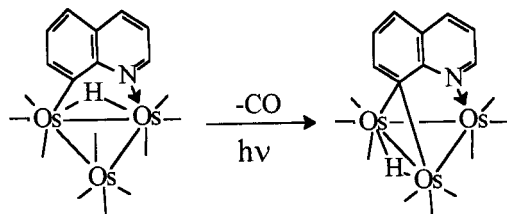
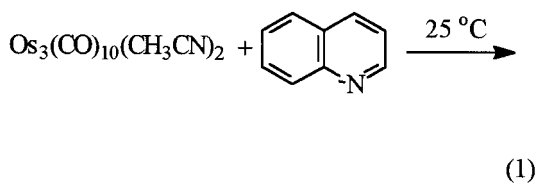
Department of Chemistry, California State University, Northridge, California 91330

Received April 9, 1999

The reactivity of  $\text{Os}_3(\text{CO})_9(\mu_3\text{-}\eta^2\text{-C}_{13}\text{H}_8\text{N})(\mu\text{-H})$  (**1**) is reported. The reaction of **1** with triphenyl phosphine gives  $\text{Os}_3(\text{CO})_9(\mu\text{-}\eta^2\text{-C}_{13}\text{H}_8\text{N})(\mu\text{-H})(\text{PPh}_3)$  (**2**), in which the phosphine is bonded to the same osmium as the C(10) of the heterocyclic ring, isostructural with the quinoline analogue. Thermal or photochemical decarbonylation of **2** gives moderate yields of  $\text{Os}_3(\text{CO})_8(\mu_3\text{-}\eta^3\text{-C}_{13}\text{H}_8\text{N})(\mu\text{-H})\text{PPh}_3$  (**3**), which has a  $\sigma\text{-}\pi$ -vinyl bonding mode with the C(9)–C(10) double bond and not the expected  $\mu_3\text{-}\eta^2$  electron-deficient bonding mode. The reactivity of **1** with hydride followed by protonation yields the electron-precise  $\text{Os}_3(\text{CO})_9(\mu_3\text{-}\eta^2\text{-C}_{13}\text{H}_9\text{N})(\mu\text{-H})_2$  (**4**), and labeling experiments using  $\text{D}^-/\text{H}^+$  indicate direct nucleophilic attack at C(9) by the deuteride followed by protonation at the metal core. The reaction of **1** with lithium isobutyryle nitrile followed by protonation gives  $\text{Os}_3(\text{CO})_9(\text{C}_{13}\text{H}_9(4\text{-(CH}_3)_2\text{CCN)N})(\mu\text{-H})$  (**5**), a result of nucleophilic addition across the 3,4 double bond. Reaction with *n*-butyllithium followed by protonation, on the other hand, gives three products,  $\text{Os}_3(\text{CO})_9(\mu_3\text{-}\eta^2\text{-C}_{13}\text{H}_8(9\text{-C}_4\text{H}_9)\text{N})(\mu\text{-H})_2$  (**6**), the result of addition at the 9-position,  $\text{Os}_3(\text{CO})_9(\mu_3\text{-}\eta^2\text{-C}_{13}\text{H}_7(6\text{-C}_4\text{H}_9)\text{N})(\mu\text{-H})$  (**7**), and  $\text{Os}_3(\text{CO})_9(\mu_3\text{-}\eta^2\text{-C}_{13}\text{H}_7(5\text{-C}_4\text{H}_9)\text{N})(\mu\text{-H})$  (**8**), both the result of nucleophilic substitution for hydrogen. The solid-state structures of **3** and **8** are reported, and the mechanistic implications of these results for the synthetic methodology being developed for these electron-deficient clusters will be discussed.

## Introduction

We have been studying the reactivity of the  $46e^-$  triosmium clusters,  $\text{Os}_3(\text{CO})_9(\mu_3\text{-}\eta^2\text{-benzoheterocycle})(\mu\text{-H})$ , which result from the reaction of  $\text{Os}_3(\text{CO})_{10}(\text{CH}_3\text{-CN})_2$  with a wide range of benzoheterocycles containing pyridinyl nitrogens (eq 1, Figure 1). The interesting



feature of these electron-deficient clusters is that on reaction with nucleophiles these species undergo reac-

tion either at the metal core or on the carbocyclic ring, depending on the nature of the nucleophile and on the substituents on the heterocycle. Thus, in the particular case of quinoline, amines and phosphines react at the metal core to give the electron-precise adducts,  $\text{Os}_3(\text{CO})_9(\mu\text{-}\eta^2\text{-C}_9\text{H}_6\text{N})(\mu\text{-H})\text{L}$ , whose structures are dependent on the nature of the ligand (eq 2).<sup>2</sup> This reactivity is essentially shut down when the strong electron-donating amino group is substituted in the 5-position only (i.e., the 3 and 6 amino derivatives still form adducts).<sup>2</sup> Hydride and a wide range of carbanions, on the other hand, react regioselectively at the 5-position to give nucleophilic addition products after acid quench (eq 3).<sup>3</sup> Substitution of the quinoline ring at the 6-position is stereoselective whereby only the *cis*-diastereomer of the addition product is obtained, while substitution at the 5-position blocks nucleophilic addition and secondary attack at the 4-position is realized (eq 4).<sup>3</sup> We are now in the process of investigating the reactivity of related electron-deficient benzoheterocycle complexes

(1) Rosenberg, E.; Arcia, E.; Kolwaite, D. S.; Hardcastle, K. I.; Ciurash, J.; Duque, R.; Gobetto, R.; Milone, L.; Osella, D.; botta, M.; Dastru', W.; Viale, A.; Fiedler, J. *Organometallics* **1998**, *17*, 415.

(2) Rosenberg, E.; Bergman, B.; Bar Din, A.; Smith, R.; Gobetto, R.; Milone, L.; Viale, A.; Dastru', W. *Polyhedron* **1998**, *17*, 2975.

(3) Bergman, B.; Holmquist, R. H.; Smith, R.; Rosenberg, E.; Hardcastle, K. I.; Visi, M.; Ciurash. *J. Am. Chem. Soc.* **1998**, *120*, 12818.

<sup>‡</sup> For parts 1–4, see refs 1–4.

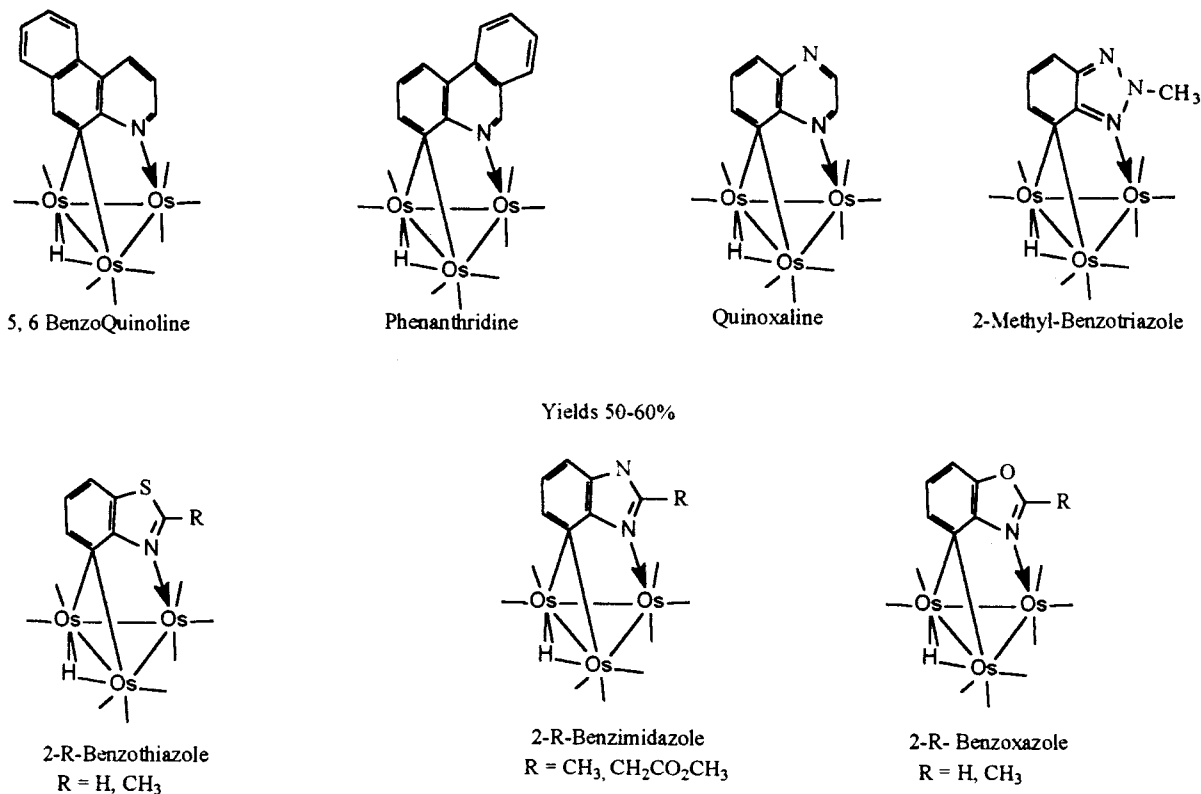
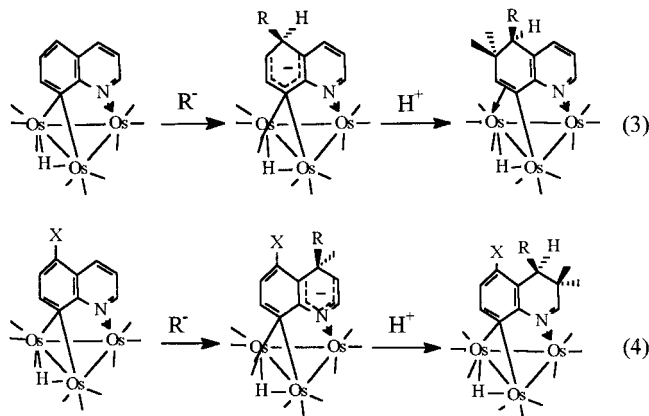
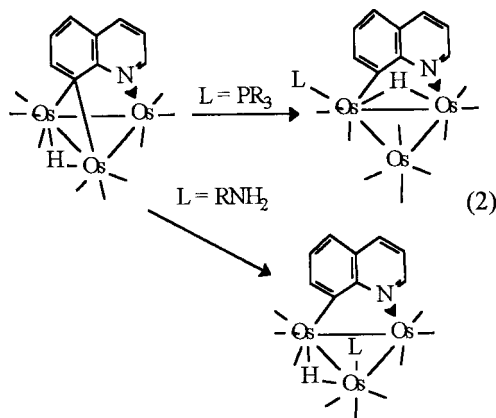


**Figure 1.**  $\mu_3\text{-}\eta^2$  electron-deficient benzoheterocycle triosmium complexes.

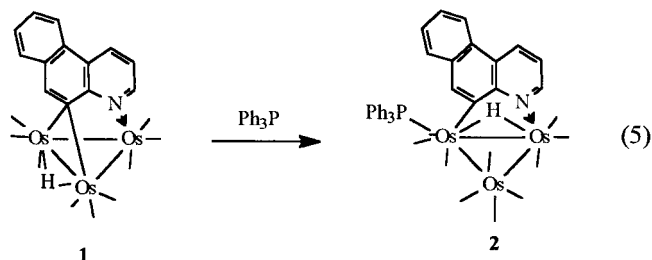


toward nucleophiles (Figure 1).<sup>4</sup> We report here the reactions of the 5,6-benzoquinoline complex  $\text{Os}_3(\text{CO})_9(\mu_3\text{-}\eta^2\text{-C}_{13}\text{H}_8\text{N})(\mu\text{-H})$  (**1**), where the 5-position of the quinoline ring system is blocked, raising the question as to what effect the presence of the third aromatic ring

will have on the course of this substrate's reactivity toward nucleophiles.

## Results and Discussion

**A. Reaction of  $\text{Os}_3(\text{CO})_9(\mu_3\text{-}\eta^2\text{-C}_{13}\text{H}_8\text{N})(\mu\text{-H})$  (**1**) with Triphenylphosphine.** We have reported the synthesis and structure of **1** previously.<sup>4</sup> The compound is obtained in sufficient yield (50% based on  $\text{Os}_3(\text{CO})_{12}$ ) to warrant a full investigation of its chemistry. The reaction of **1** with triphenylphosphine proceeds quantitatively to yield a single product,  $\text{Os}_3(\text{CO})_9(\mu_3\text{-}\eta^2\text{-C}_{13}\text{H}_8\text{N})(\mu\text{-H})\text{PPh}_3$  (**2**), whose structure can be assigned to an adduct having the phosphine substituted on the same osmium atom as C(10) of the heterocyclic ring (eq 5).<sup>1</sup> This assignment is based on the <sup>13</sup>C NMR of a

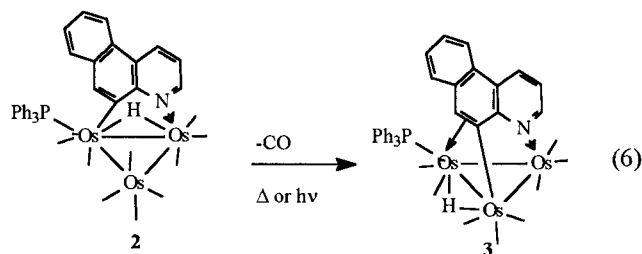


<sup>13</sup>CO-enriched sample of **2** whose spectrum in the carbonyl region shows nine resonances, which can be assigned on the basis of known trends for this type of triosmium carbonyl cluster.<sup>1,5</sup> Two phosphorus-coupled resonances at 182.53 (<sup>2</sup>J<sup>13</sup>P-<sup>13</sup>C = 4.6 Hz) and 185.64-

(4) Abedin, Md. J.; Bergman, B.; Holmquist, R.; Smith, R.; Rosenberg, E.; Ciruash, J.; Hardcastle, K.; Roe, J.; Vazquez, V.; Roe, C.; Kabir, S.; Roy, B.; Alam, S.; Azam, K. A. *Coord. Chem. Rev.*, in press.

( $^2J^{31P-13C} = 6.2$  Hz) ppm are observed. The proton-coupled spectrum reveals that the resonance at 182.53 ppm collapses to a doublet of doublets ( $^2J^{1H-13C} = 9.0$  Hz), while the more downfield resonance shows an unresolved hydride-carbonyl coupling. We can thus assign these resonances to the radial and axial carbonyls on the same osmium atom as the phosphorus respectively based on the observed couplings and their relative chemical shifts. Two resonances at 178.10 ( $^2J^{1H-13C} = 13$  Hz) and 177.93 ( $^2J^{1H-13C} = 4.5$  Hz) ppm can be assigned to the radial carbonyl *trans* and *cis* to the hydride which bridges the same edge as the heterocycle. The placement of the phosphorus on the same osmium atom as that bound to carbon is based on the fact that in complexes of this type the carbonyl *trans* to the hydride on the nitrogen-bound osmium always shows a larger coupling constant than the one on the carbon-bound osmium atom.<sup>5,6</sup> This trend has been observed in a wide range of compounds and for the quinoline analogue of **2**, for which a crystal structure has been obtained.<sup>1</sup> Three of the remaining five resonances at 176.50, 178.02, and 184.43 ppm show no resolvable hydride or phosphorus coupling but are slightly broadened at room temperature and sharpen as the temperature is lowered to 0 °C. We can assign these resonances to three of the four carbonyls, two radial and one axial on the Os(CO)<sub>4</sub> group in **2**, which are just beginning to undergo tripodal motion on the Os(CO)<sub>4</sub> groups in this type of cluster.<sup>5</sup> The two remaining resonances at 177.06 and 184.50 ppm are interchangeably assigned to the other axial carbonyl on the Os(CO)<sub>4</sub> group and the one nitrogen-bound osmium atom. The structure of **2** is identical with its quinoline analogue.<sup>1</sup>

Thermolysis or photolysis of **2** leads to the formation of an electron-precise,  $\sigma$ - $\pi$ -vinyl complex involving the C(9)-C(10) double bond, Os<sub>3</sub>(CO)<sub>8</sub>( $\mu_3$ - $\eta^3$ -C<sub>13</sub>H<sub>8</sub>N)( $\mu$ -H)PPh<sub>3</sub> (**3**, eq 6). The assignment of this structure is based



on a solid-state structural investigation, and the <sup>1</sup>H NMR data indicate that this structure persists in solution.

The solid-state structure of **3** is shown in Figure 2, crystal data are given in Table 1, and selected distances and bond angles are given in Table 2. The structure consists of an Os<sub>3</sub> triangle with three significantly different metal-metal bond lengths, the shortest being the edge bridged by the nitrogen atom and  $\sigma$ -bound to C(10) (Os(2)-Os(3) = 2.768(8) and Os(3)-C(10) =

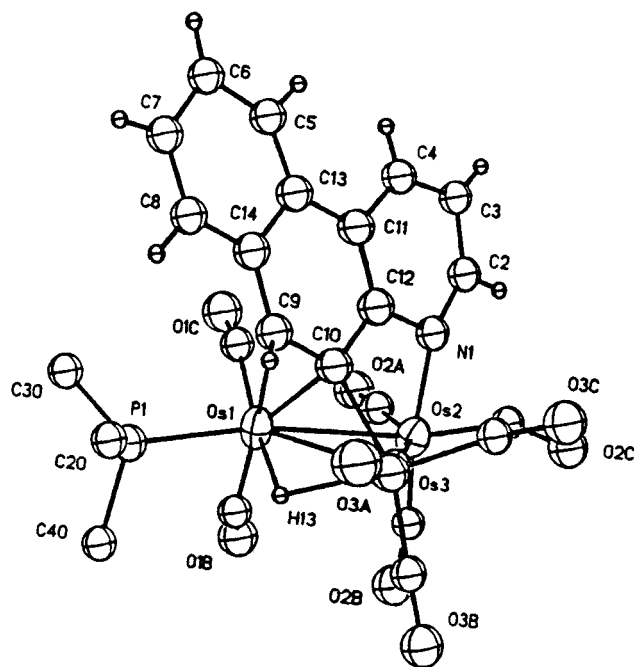


**Figure 2.** Solid-state structure of Os<sub>3</sub>(CO)<sub>8</sub>( $\mu_3$ - $\eta^3$ -C<sub>13</sub>H<sub>8</sub>N)-( $\mu$ -H)PPh<sub>3</sub> (**3**) showing the calculated position of the hydride.

2.05(7) Å); the longest edge (Os(1)-Os(2) = 2.917(8) Å) is bridged by the nitrogen atom and the  $\pi$ -bonds to Os(1) (Os(1)-C(10) = 2.02(4) and Os(1)-C(9) = 2.050(7) Å). It seems reasonable to suggest that these relatively disparate metal-metal bond lengths are imposed by the requirements of the  $\sigma$ - $\pi$ -bonding mode and the rigidity of the 5,6-benzoquinoline ring. The doubly bridged edge is intermediate in length (Os(1)-Os(3) = 2.844(8) Å). This overall trend in relative bond lengths is similar to that observed in the more flexible  $\sigma$ - $\pi$ -vinyl 5,6-dihydroquinoline analogues of **3**.<sup>1,3</sup> The metal-carbon  $\sigma$  and  $\pi$  bond lengths are also shorter on average in **3** than in that series of complexes (average bond lengths are 2.14 Å for the  $\sigma$  bond and 2.32 Å for the  $\pi$  bonds). The average C-C bond lengths in the two benzenoid rings are normal (1.39(5) Å), and the C(9)-C(10) is in the range for an isolated metal-coordinated double bond (1.35(9) Å); but the large errors in these bond lengths make it difficult to draw any firm conclusions from these data.

The chemical shift of the hydrogen on C(9) (5.75 ppm) is considerably to lower field than the vinyl hydrogens in related 5,6-dihydroquinoline  $\sigma$ - $\pi$ -vinyl complexes (~4.0 ppm), indicating some retention of aromatic character in the central ring.<sup>3</sup> Broad band modulated phosphorus decoupling of the proton spectrum collapses the doublet resonance at 5.75 ppm ( $^2J^{31P-1H} = 5.6$  Hz) to a singlet, while the other hydrocarbon resonances remain unchanged. This result indicates that the  $\sigma$ - $\pi$ -vinyl structure remains unchanged in solution and puts an upper limit of 35.2 s<sup>-1</sup> ( $< 2\pi J$ ) on the rate of  $\sigma$ - $\pi$ -interchange. This is in sharp contrast to the 5,6-dihydroquinoline complex in which the  $\sigma$ - $\pi$  interchange is rapid on the NMR time scale at room temperature.

The quinoline analogue of **2** does not give a  $\mu_3$ - $\eta^3$   $\sigma$ - $\pi$ -vinyl complex on thermolysis or photolysis. Indeed, only nonspecific decomposition and phosphine ligand dissociation to give the unsubstituted nona- and decacar-

(5) Rosenberg, E.; Day, M.; Espitia, D.; Hardcastle, K. I.; Kabir, S. E.; McPhillips, T.; Gobetto, R.; Milone, L.; Osella, D. *Organometallics* **1993**, *12*, 2390.

(6) Rosenberg, E.; Hardcastle, K. I.; Kabir, S. E.; Milone, L.; Gobetto, R.; Botta, M.; Nishimura, N.; Yin, M. *Organometallics* **1995**, *14*, 3068.

**Table 1. Crystal Data and Structure Refinement of 3 and 7**

	3	7
empirical formula	C <sub>39</sub> H <sub>24</sub> NO <sub>8</sub> Os <sub>3</sub> P	C <sub>26</sub> H <sub>17</sub> NO <sub>9</sub> Os <sub>3</sub>
fw	1236.16	1058.01
temperature	293(2) K	293(2) K
wavelength	0.71073 Å	0.71073 Å
crystal system	monoclinic	monoclinic
space group	<i>P2</i> <sub>1</sub> / <i>c</i>	<i>P2</i> <sub>1</sub> / <i>n</i>
unit cell dimensions	<i>a</i> = 11.144(10) Å <i>b</i> = 16.148(12) Å, $\beta$ = 99.24(9)° <i>c</i> = 20.029(14) Å	<i>a</i> = 9.9783(6) Å <i>b</i> = 12.8751(8) Å, $\beta$ = 92.588(1)° <i>c</i> = 21.8259(13) Å
volume, <i>Z</i>	3558(6) Å <sup>3</sup> , 4	2801.1(3) Å <sup>3</sup> , 4
density (calcd)	2.308 Mg/m <sup>3</sup>	2.509 Mg/m <sup>3</sup>
abs coeff	10.789 mm <sup>-1</sup>	13.626 mm <sup>-1</sup>
<i>F</i> (000)	2288	1920
crystal size	0.15 × 0.05 × 0.05 mm	0.15 × 0.10 × 0.05 mm
$\theta$ range for data collection	1.63–17.99°	1.84–28.28°
limiting indices	−9 ≤ <i>h</i> ≤ 9, 0 ≤ <i>k</i> ≤ 14, −17 ≤ <i>l</i> ≤ 17	−13 ≤ <i>h</i> ≤ 13, −17 ≤ <i>k</i> ≤ 16, −29 ≤ <i>l</i> ≤ 28
no. of reflns cold	7534	29149
no. of indep reflns	2444 ( <i>R</i> <sub>int</sub> = 0.0000)	6537 ( <i>R</i> <sub>int</sub> = 0.0612)
abs corr	none	SADABS Bruker AXS
refinement method	full-matrix least-squares on <i>F</i> <sup>2</sup>	full-matrix least-squares on <i>F</i> <sup>2</sup>
no. of data/restraints/params	2246/82/182	6535/8/350
goodness-of-fit on <i>F</i> <sup>2</sup>	1.398	0.916
final <i>R</i> indices [ <i>I</i> > 2σ( <i>I</i> )]	<i>R</i> 1 = 0.1198, <i>wR</i> 2 = 0.2473	<i>R</i> 1 = 0.0392, <i>wR</i> 2 = 0.0811
<i>R</i> indices (all data)	<i>R</i> 1 = 0.1932, <i>wR</i> 2 = 0.4268	<i>R</i> 1 = 0.0758, <i>wR</i> 2 = 0.0919
extinction coeff	1.35(4)	0.00031(4)
largest diff peak and hole	1.919 and −1.065 e Å <sup>-3</sup>	1.702 and −1.429 e Å <sup>-3</sup>

**Table 2. Selected Distances (Å) and Angles(deg) for 3<sup>a</sup>**

Distances			
Os(1)–Os(2)	2.917(8)	C(9)–C(10)	1.375(4)
Os(1)–Os(3)	2.844(8)	C(9)–C(14)	1.375(4)
Os(2)–Os(3)	2.768(8)	C(10)–C(12)	1.375(4)
Os(1)–C(9)	2.50(4)	C(12)–N(1)	1.424(4)
Os(1)–C(10)	2.02(4)	C(11)–C(12)	1.375(4)
Os(1)–P(1)	2.37(3)	C(13)–C(14)	1.375(4)
Os(3)–C(10)	2.05(7)	C(2)–C(3)	1.375(4)
Os(2)–N	2.01(2)	C–O <sup>b</sup>	1.20(5)
Os–CO <sup>b</sup>	1.82(4)		

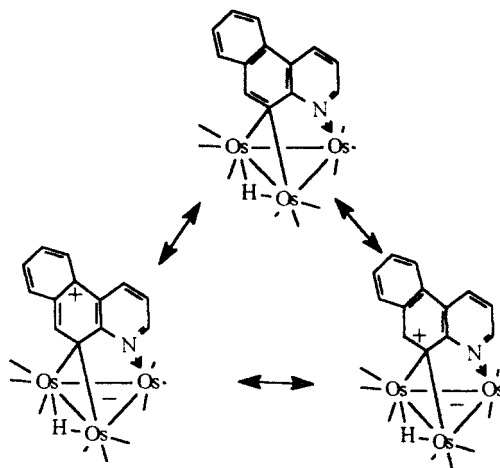
Angles			
Os(1)–Os(2)–Os(3)	60.07(14)	C(9)–C(10)–C(12)	110.0(4)
Os(1)–Os(3)–Os(2)	62.43(13)	C(11)–C(12)–N(1)	130.7(3)
Os(2)–Os(1)–Os(3)	57.50(12)	C(2)–N(1)–C(12)	105.1(4)
Os(3)–Os(1)–C(9)	72.17(2)	N(1)–C(2)–C(13)	133.0(3)
Os(3)–Os(1)–C(10)	52.1(2)	C(2)–C(3)–C(4)	110.6(3)
Os(1)–Os(3)–C(10)	41.2(2)	C(4)–C(11)–C(12)	112.7(3)
Os(3)–Os(2)–N(1)	82.5(2)	C(11)–C(13)–C(14)	111.9(3)
Os(1)–Os(2)–N(1)	85.0(2)	C(15)–C(13)–C(14)	132.1(3)
Os–C–O <sup>b</sup>	167(6)		

<sup>a</sup> Numbers in parentheses are average standard deviations.

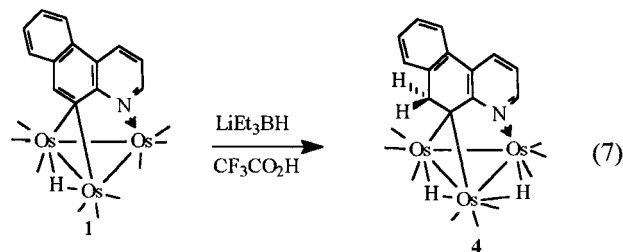
<sup>b</sup> Average values.

bonyl precursors of the quinoline complex are obtained. Thus, phosphine substitution apparently prevents formation of the  $\mu_3\text{-}\eta^2$  electron-deficient bonding mode upon thermolysis or photolysis of the electron-precise precursors.<sup>1</sup> We have previously shown that the reverse reaction (i.e., carbonylation of the 46e<sup>−</sup> electron cluster) results in a migration of the heterocyclic ligand to a different edge of the metal triangle.<sup>1</sup> From microscopic reversibility, we can infer this process is also occurring during decarbonylation. It may be that the presence of the bulky phosphine on the osmium atom bound to C(10) in **2** (C(8) in the quinoline analogue) prevents this ligand migration by increasing the metal carbon bond strength or by steric crowding in the transition state or in the product.

**B. Reaction of 1 with Nucleophiles.** The electron-deficient  $\mu_3\text{-}\eta^2$  quinoline triosmium complexes undergo regioselective nucleophilic attack at the 5-position with

**Scheme 1. Resonance Structures for 1**

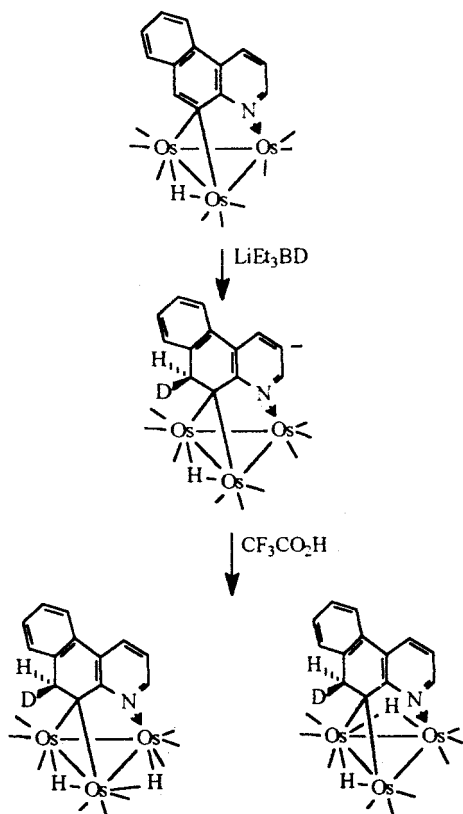
hydride donors. In the case of **1**, the 5-position is blocked, and according to the contributions to the electron distribution from the expected resonance structures, the 9-position of the 5,6-benzoquinoline ring should be the secondary site of nucleophilic attack (Scheme 1). Indeed, this is the case for **1**, where initial attack by hydride followed by protonation yields the electron-precise cluster Os<sub>3</sub>(CO)<sub>9</sub>( $\mu_3\text{-}\eta^2\text{-C}_{13}\text{H}_9\text{N}$ )( $\mu\text{-H}$ )<sub>2</sub> (**4**, eq 7). That initial attack by H<sup>−</sup> is indeed at the



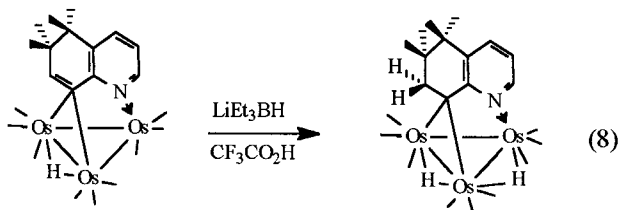
9-position is verified by the reaction of **1** with D<sup>−</sup>/H<sup>+</sup>, where no deuterium is incorporated into the hydrides and where the two doublets at 3.89 and 3.22 ppm (<sup>2</sup>*J* =



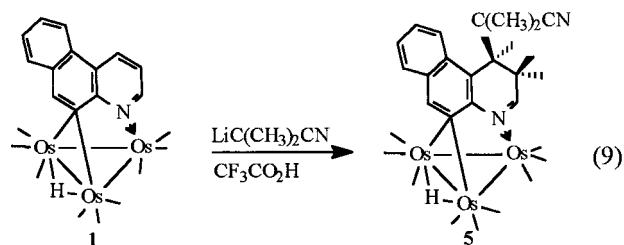
## Scheme 2. Hydride Attack on 1



15.0 Hz) assigned to the hydrogens on C(9) appear as sharp singlets of relative intensity of 0.5 each. The hydride region appears as a singlet at  $-14.20$  ppm and two singlets at  $-14.746$  and  $-14.753$  (rel int = 1:0.5:0.5), which can be understood in terms of the presence of the two expected isotopomers formed which differ with respect to the position of one bridging hydride relative to the deuteride on C(9) (Scheme 2). Although we cannot rigorously exclude a short-lived dihydride anion intermediate with preferential deuterium transfer to C(9), resulting from a thermodynamic isotope effect, one would expect some incorporation of hydrogen into the C(9) position, which is not observed. The intermediate anion (Scheme 2) shows a single hydride resonance at  $-14.38$  ppm. This pattern of reactivity with  $D^-/H^+$  is analogous to that observed for the 5,6-dihydroquinoline complexes (eq 8).

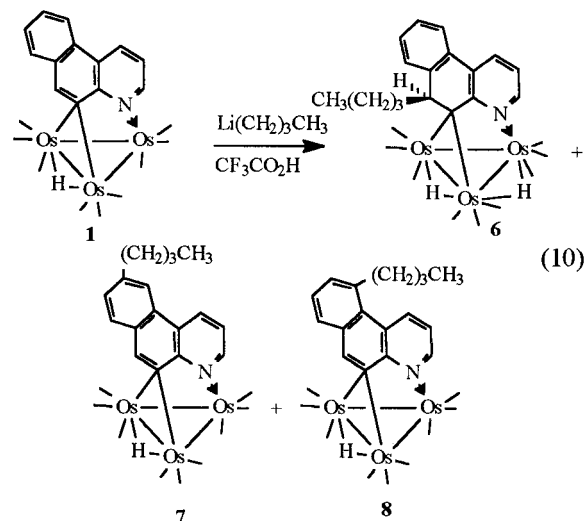


The reaction of **1** with  $Li(CH_3)_2CCN$  yields one major product,  $Os_3(CO)_9(\mu_3-\eta^2-C_{13}H_9(4-(CH_3)_2CCN)N)(\mu-H)$  (**5**), in good yield (eq 9, 58%). The structure of the product is based on  $^1H$  NMR, infrared, and elemental analysis. The key features of the  $^1H$  NMR data that define the structure of **5** are (1) four strongly coupled ( $^1H$  COSY) aromatic resonances assigned to the hydrogens on C(5)–C(8); (2) a singlet resonance at 8.08 ppm assigned to the proton on C(9); (3) a multiplet of relative intensity



two at 3.18 ppm which is strongly coupled ( $^1H$  COSY) to the most downfield resonance at 8.89 ppm assigned to the hydrogen on C(2) and to an aliphatic resonance at 3.90 ppm assigned to the hydrogen on C(4). The presence of the isobutyryl group is indicated by the observation of two diastereotropic methyls at 1.38 and 1.24 ppm. The same coupling pattern between the most downfield resonance and the aliphatic protons is observed for the nucleophilic addition product obtained from the reaction of  $Os_3(CO)_9(\mu_3-\eta^2-C_9H_5(5-Cl)N)(\mu-H)$  with  $LiC(CH_3)_2CN$ , where the 5-position is blocked as in **1** and nucleophilic addition takes place across the 3,4 double bond.<sup>3</sup>

The reaction of **1** with  $Li^iBu$  takes a completely different course. Three products are obtained in approximately equal yield:  $Os_3(CO)_9(\mu_3-\eta^2-C_{13}H_8(9-(CH_2)_3-CH_3)N)(\mu-H)_2$  (**6**) and two green isomers having the formula  $Os_3(CO)_9(\mu_3-\eta^2-C_{13}H_7(5- \text{or } 6-(CH_2)_3CH_3)N)(\mu-H)$  (**7** and **8**, eq 10). Compound **6** could be readily



identified from its  $^1H$  NMR, which showed two hydride doublets at  $-14.28$  and  $-15.02$  ppm ( $^2J = 1.2$  Hz), a doublet of doublets at 2.78 ppm, which is coupled to two of the  $^iBu$  methylene hydrogens at 1.45 and 1.06 ppm. Seven aromatic resonances are observed, which are divided into a group of three and a group of four by  $^1H$  COSY experiments.

Compounds **7** and **8** each showed a single hydride resonance at  $-13.55$  and  $-12.97$  ppm, respectively. Both show a singlet aromatic resonance at 8.11 and 8.67 ppm, which we can assign to the hydrogen on C(9). Compound **7** shows an additional singlet at 7.90 ppm, a set of two aromatic resonances, and a set of three aromatic resonances by  $^1H$  COSY experiments. Compound **8** shows two sets of three aromatic resonances. These data support a structure for compound **7** where the  $^iBu$  group

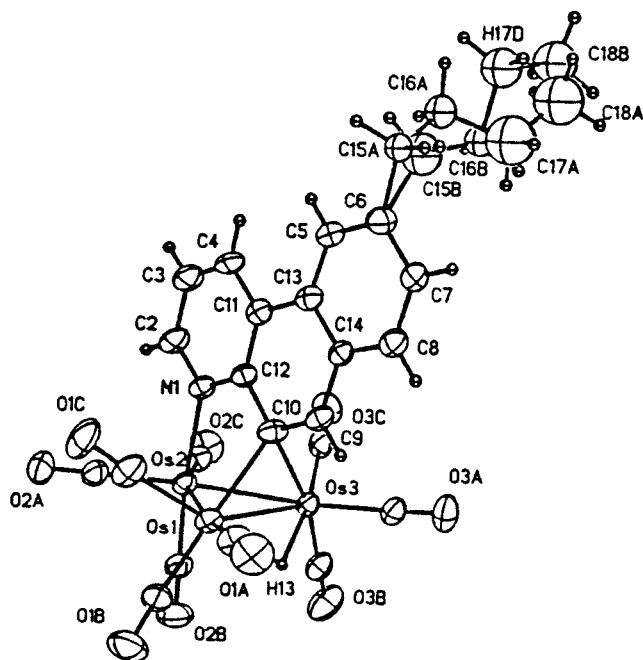


**Figure 3.** Solid-state structure of  $(\mu_3\text{-}\eta^2\text{-C}_{13}\text{H}_7(6\text{-}^n\text{Bu})\text{N})(\mu\text{-H})$  (**7**) showing the calculated position of the hydride.

**Table 3. Selected Distances (Å) and Bond Angles (deg) for 7<sup>a</sup>**

Distances			
Os(1)–Os(2)	2.781(1)	C(9)–C(10)	1.37(1)
Os(1)–Os(3)	2.776(1)	C(10)–C(12)	1.45(1)
Os(2)–Os(3)	2.794(1)	C(9)–C(14)	1.42(1)
Os(1)–C(10)	2.25(1)	C(12)–N(1)	1.37(1)
Os(3)–C(10)	2.31(1)	C(2)–N(1)	1.33(1)
Os(2)–N(1)	2.18(1)	C(6)–C(15) <sup>b</sup>	1.52(1)
Os–CO <sup>b</sup>	1.90(1)	C–O <sup>b</sup>	1.13(1)
Angles			
Os(1)–Os(2)–Os(3)	59.74(1)	C(9)–C(10)–C(12)	116.(1)
Os(1)–Os(3)–Os(2)	59.91(1)	C(12)–N(1)–C(2)	120.(1)
Os(2)–Os(1)–Os(3)	60.36(1)	C(10)–C(9)–C(14)	125.(1)
Os(1)–Os(3)–C(10)	51.5(2)	C(10)–C(12)–C(11)	122.(1)
Os(3)–Os(1)–C(10)	53.3(2)	N(1)–C(12)–C(11)	120.(1)
Os(1)–Os(2)–N(1)	85.2(2)	N(1)–C(2)–C(3)	121.(1)
Os(3)–Os(2)–N(1)	84.2(2)	C(12)–C(11)–C(4)	119.(1)
Os–C–O <sup>b</sup>	177(1)	C(2)–C(3)–C(4)	120.(1)

<sup>a</sup> Numbers in parentheses are average standard deviations.

<sup>b</sup> Average values.

has substituted for hydrogen on either C(6) or C(7) and for compound **8**, substitution on C(5) or C(8).

We were able to obtain crystals for **7** which were suitable for single-crystal X-ray diffraction study. The solid-state structure of **7** is shown in Figure 3, crystal data are given in Table 1, and selected distances and bond angles are given in Table 3. The structure consists of an essentially equilateral triangle of osmium atoms. The 5,6-benzoquinoline ring is bound to the metal core in a  $\mu_3\text{-}\eta^2$  fashion, and the osmium ligand bond lengths (Os(1)–C(10) = 2.25(1) Å, Os(3)–C(10) = 2.31(1) Å, Os(2)–N(1) = 2.18(1) Å) are very similar to those found in **1** (Os(1)–C(10) = 2.25(1), Os(3)–C(10) = 2.32(1) Å, Os(2)–N(1) = 2.14(1) Å).<sup>4</sup> The <sup>n</sup>Bu group is located on C(6) and is disordered in the structure. The C(14)–C(6) bond length is a normal C–C single bond at 1.52(1) Å, and the C(5)–C(6) and C(6)–C(7) bonds are typical of aromatic C–C bonds at 1.37(1) and 1.41(1) Å.

Although we cannot definitely assign the structure of **8**, we tentatively assign it to a C(5)-<sup>n</sup>Bu-substituted

derivative based on the fact that both **7** and **8** have resonances at 7.90 and 8.25 ppm, respectively, which we can assign to C(8) in both compounds on the basis of <sup>1</sup>H COSY NMR. Additionally, C(5) would be the expected site of nucleophilic attack if the electron deficiency is primarily communicated to the positions ortho and para to the carbon atom involved in electron-deficient bonding to the metal core (Scheme 1). Although we cannot be certain of the mechanism by which **7** and **8** are formed, it seems reasonable to propose that initial nucleophilic attack at the 5- and 6-positions, respectively, is followed by hydride abstraction during the proton quench. We have previously noted spontaneous rearomatization after acid quench in the reactions of carbanions with these types of complexes.<sup>3</sup>

## Conclusions

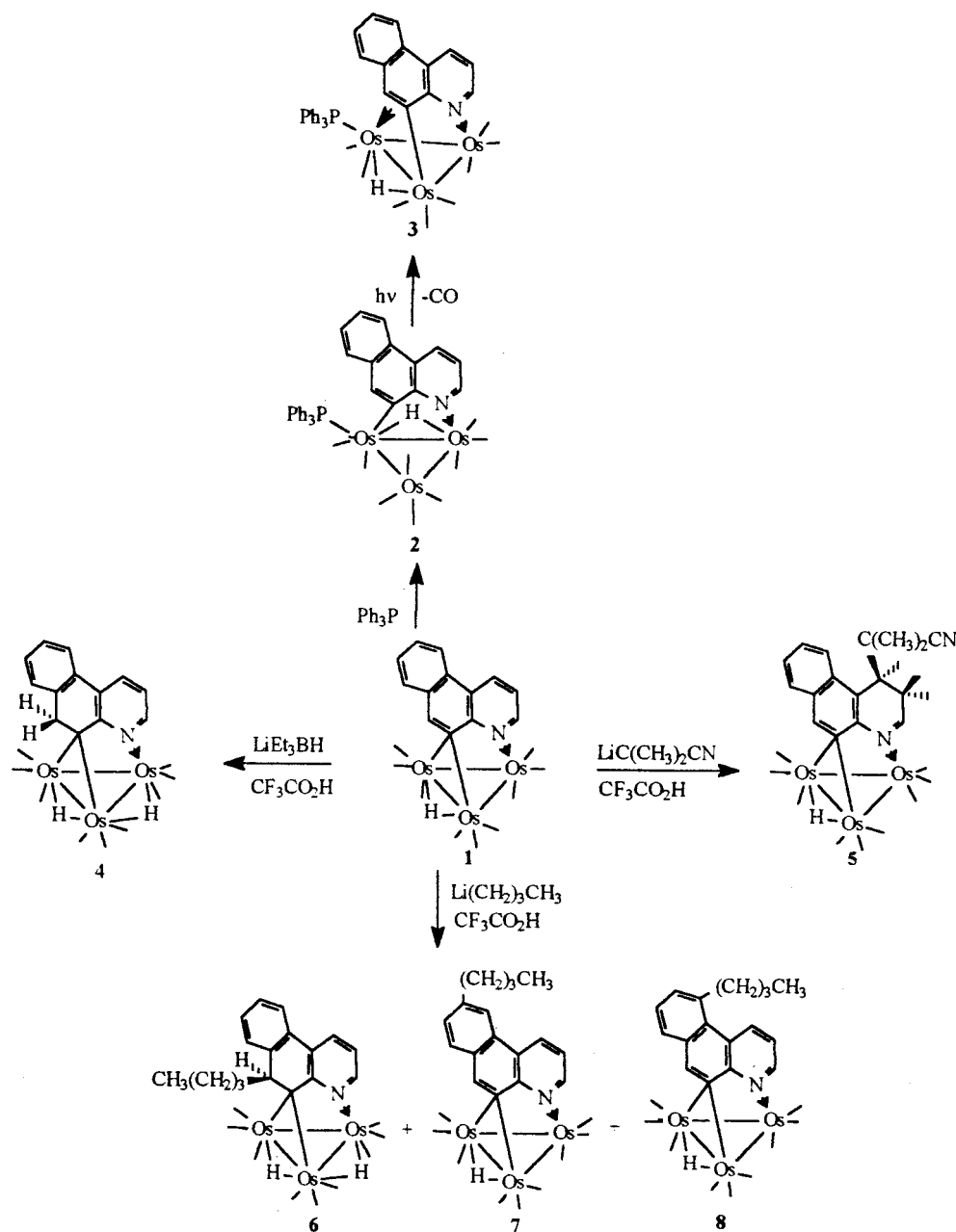
The reactions of **1** reported here, which are summarized in Scheme 3, reveal several special features of the 5,6-dibenzoquinoline ring system relative to its quinoline analogue. First, whereas the attempted decarbonylation of Os<sub>3</sub>(CO)<sub>9</sub>( $\mu\text{-}\eta^2\text{-C}_9\text{H}_6\text{N})(\mu\text{-H})\text{PPh}_3$  yields only Os<sub>3</sub>(CO)<sub>n</sub>( $\mu_m\text{-}\eta^2\text{-C}_9\text{H}_6\text{N})(\mu\text{-H})$  ( $n = 9$  or  $10$ ,  $m = 2$  or  $3$ ) and nonspecific decomposition, the thermolysis of **2** yields **3**, where the formation of two benzenoid aromatic rings allows isolation of a stable  $\sigma\text{-}\pi$ -vinyl complex. In the case of the quinoline complex, formation of such a bonding mode would require disruption of this benzo-heterocycle's aromaticity.

Similarly, in the case of nucleophilic attack on **1**, attack at the 9-position by hydride or Li<sup>n</sup>Bu is probably also driven, at least in part, by the formation of the two benzenoid aromatic centers. This is our first observation of nucleophilic attack at what would be C(7) in the case of the quinoline analogues. Our initial thought was that this position is sterically blocked, but the results reported here seem to suggest that initial attack at the 5-position by small nucleophiles may be preferred for electronic reasons in the case of the quinoline complexes. There is, of course, a significant steric component to the regiochemistry observed since the bulkier LiC(CH<sub>3</sub>)<sub>2</sub>CN attacks only at C(4). We have no explanation at present as to why secondary attack by Li<sup>n</sup>Bu on **1** is at C(5) and C(6) rather than C(4). It is tempting to suggest that the electron deficiency felt at C(13) is transferred to these positions, but this does not explain why LiC(CH<sub>3</sub>)<sub>2</sub>CN does not attack at C(6), which is not sterically encumbered. Studies of the reactivity of related benzo-heterocycles and calculations aimed at revealing the details of electron distributions in these complexes are currently under way in our laboratories.

## Experimental Section

**Materials.** All reactions were performed in an atmosphere of prepurified nitrogen, but were worked up in air. Acetonitrile and methylene chloride were distilled from calcium hydride before use, and tetrahydrofuran was distilled from benzophenone ketyl. Osmium carbonyl was purchased from Strem Chemical and used as received. 5,6-Benzoquinoline, isobutyronitrile, lithium triethylborohydride, trifluoroacetic acid, triphenylphosphine, diisopropylamine, and Li<sup>n</sup>Bu were purchased from Aldrich Chemical and used as received. Compound **1** and LiC(CH<sub>3</sub>)<sub>2</sub>CN were prepared according to literature

Scheme 3. Summary of the Reactivity of 1



procedures.<sup>3,4</sup>  $\text{Os}_3(\text{CO})_{10}(\text{CH}_3\text{CN})_2$  was prepared according to literature procedures.<sup>7</sup>

**Spectra.**  $^1\text{H}$  and  $^{13}\text{C}$  NMR were recorded on a Varian Unity Plus 400 at 400 and 100 MHz, respectively. Chemical shifts are reported downfield positive with respect to tetramethylsilane and, the magnitudes of coupling constants are reported for only those that are relevant to the structural identification of the compounds reported. Infrared spectra were recorded on a Perkin-Elmer 1600 FT-IR spectrometer. Elemental analyses were performed by Schwarzkopf Microanalytical Laboratories, Woodside, NY.

**Synthesis of  $\text{Os}_3(\text{CO})_9(\mu\text{-}\eta^2\text{-C}_{13}\text{H}_8\text{N})(\mu\text{-H})\text{PPh}_3$  (2).** Compound 1 (21 mg, 0.02 mmol) was dissolved in 15 mL of  $\text{CH}_2\text{Cl}_2$  under nitrogen, and triphenylphosphine (10 mg, 0.04 mmol) in 2 mL of  $\text{CH}_2\text{Cl}_2$  was injected into the solution by syringe. After 5 min the solution turned from dark green to orange-yellow. The solution was run through a short silica gel column,

to remove excess triphenylphosphine as a fore run, and then concentrated to  $\sim 3$  mL. To the orange-yellow solution was added  $\sim 3$  mL hexanes and the product recrystallized at  $-20$  °C to yield 24 mg (100%) of  $\text{Os}_3(\text{CO})_9(\mu\text{-}\eta^2\text{-C}_{13}\text{H}_8\text{N})(\mu\text{-H})\text{PPh}_3$  (2).

**Spectroscopic and Analytical Data for 2.** Anal. Calcd for  $\text{C}_{40}\text{H}_{24}\text{NO}_9\text{Os}_3\text{P}$ : C, 38.0; H, 1.91; N, 1.10. Found: C, 37.54, H, 2.07; N, 1.04. IR ( $\nu$  CO) in hexane: 2086(w), 2044(s), 2027(s), 2010(s), 1992(m), 1976(w), 1968(w), 1960(w), 1944(w)  $\text{cm}^{-1}$ .  $^1\text{H}$  NMR in  $\text{CDCl}_3$ :  $\delta$  9.44 (d, H(2)), 8.91 (d, H(4)), 8.31 (d, H(8)), 7.92 (s, H(9)), 7.41 (dd, H(6)), 7.36 (dd, H(7)), 7.10–7.20 (m, 15 H), 7.16 (dd, H(3)), 7.10 (d, H(5)),  $-11.63$  (d,  $J^{\text{P-H}} = 15.6$  Hz, hydride).  $^{13}\text{C}$  NMR ( $\text{CDCl}_3$ ):  $\delta$  185.64 ( $^2J^{\text{P-C}} = 6.2$  Hz), 184.50, 184.43, 182.53 ( $^2J^{\text{P-C}} = 4.6$  Hz), 178.10 ( $^2J^{\text{H-C}} = 13$  Hz), 178.02, 177.93 ( $^2J^{\text{H-CO}} = 4.5$  Hz), 177.06, 176.50.  $^{31}\text{P}$  NMR in  $\text{CDCl}_3$ :  $\delta$  12.37 relative to external  $\text{H}_3\text{PO}_4$  in  $\text{CDCl}_3$ .

**Synthesis of  $\text{Os}_3(\text{CO})_8(\mu\text{-}\eta^3\text{-C}_{13}\text{H}_8\text{N})(\mu\text{-H})\text{PPh}_3$  (3).** Compound 2 (97 mg 0.07 mmol) was dissolved in 35 mL of  $\text{CH}_2\text{Cl}_2$  in a quartz reaction vessel, and the yellow-orange solution was

(7) Lewis, J.; Dyson, P. J.; Alexander, B. J.; Johnson, B. F. G.; Martin, C. M.; Nairn, J. G. M.; Parsini, E. *J. Chem. Soc., Dalton Trans.* **1993**, 981.



photolyzed under a slow bubble of N<sub>2</sub> in a Rayonet photochemical reactor equipped with 3000 Å lamps. After 1 h and 15 min, the reaction solution was evaporated to dryness, taken up in a minimum amount of methylene chloride, and purified by thin-layer chromatography using 30:70 CH<sub>2</sub>Cl<sub>2</sub>/hexane as eluent. Two major bands were eluted in addition to minor amounts of **1** and its decacarbonyl precursor. The faster moving yellow band contained unreacted **2** (51 mg), and the slower moving brown band contained **3** (29 mg, 63% based on consumed **2**). Longer photolysis times led to lower yields owing to the photosensitivity of **3**.

**Spectroscopic and Analytical Data for 3.** Anal. Calcd for C<sub>39</sub>H<sub>24</sub>O<sub>8</sub>Os<sub>3</sub>NP: C, 37.9; H, 1.95; N, 1.13. Found: C, 38.35; H, 2.15, N, 1.25. IR (ν CO) in hexane: 2078(m), 2042(s), 2026(s), 2010(s), 1994(m), 1986(w), 1968(w), 1960(w) cm<sup>-1</sup>. <sup>1</sup>H NMR in CDCl<sub>3</sub>: δ 8.95 (d, H(2)), 8.53 (d, H(4)), 8.14 (d, H(8)), 7.58 (dd, H(7)), 7.29, 7.42 (m, 15 H), 7.18 (dd, H(7)), 7.05 (dd, H(3)), 6.61 (d, H(5)), 5.75 (d, <sup>3</sup>J<sup>31</sup>P–<sup>1</sup>H=5.6 Hz, H(9)), –13.69 (d, <sup>2</sup>J<sup>31</sup>P–<sup>1</sup>H=8.8 Hz, hydride).

**The Synthesis of Os<sub>3</sub>(CO)<sub>9</sub>(μ<sub>3</sub>-η<sup>2</sup>-C<sub>13</sub>H<sub>9</sub>N)(μ-H)<sub>2</sub>(**4**).** Compound **1** (51.5 mg, 0.051 mmol) was dissolved in 15 mL of CH<sub>2</sub>Cl<sub>2</sub> under N<sub>2</sub>, and 50 μL of 1.0 M solution of Et<sub>3</sub>BXLi (X = H or D) was added dropwise to the stirred solution by syringe. The mixture was allowed to stir for 20 min, and CF<sub>3</sub>SO<sub>3</sub>H (4.9 μL, 0.06 mmol) was added. The yellow-orange solution was stirred for 5 min and then rotary evaporated, and the residue was taken up in minimum CH<sub>2</sub>Cl<sub>2</sub> and separated by preparative TLC using 35:65 CH<sub>2</sub>Cl<sub>2</sub>/hexanes. The fastest moving yellow band yielded 28 mg (82% based on consumed **1**), and the slower moving green band contained 17 mg of **1**.

**Spectroscopic and Analytical Data for 4.** Anal. Calcd for C<sub>22</sub>H<sub>11</sub>O<sub>9</sub>Os<sub>3</sub>N: C, 26.32; H, 1.10; N, 1.40. Found: C, 25.86; H, 1.04; N, 1.37. IR (ν CO) in hexane: 2096(m), 2073(s), 2045(s), 2016(s), 2002(m), 1992(m), 1978(w), 1970(w) cm<sup>-1</sup>. <sup>1</sup>H NMR in CDCl<sub>3</sub>: δ 8.21 (d, H(2)), 7.91 (d, H(4)), 7.48 (d, H(8)), 7.29 (m, 2H, H(6) and H(7)), 7.07 (d, H(5)), 6.63 (dd, H(3)), 3.90 (d, <sup>2</sup>J<sup>1</sup>H–<sup>1</sup>H = 14.4 Hz, H(9)), 3.22 (d, <sup>1</sup>J<sup>1</sup>H–<sup>1</sup>H = 14.4 Hz, H<sup>1</sup>C(9)), –14.20 (s, hydride), –14.75 (s, hydride).

**The Synthesis of Os<sub>3</sub>(CO)<sub>9</sub>(μ<sub>3</sub>-η<sup>2</sup>-C<sub>13</sub>H<sub>9</sub>(4-C(CH<sub>3</sub>)<sub>2</sub>CN)N)(μ-H) (**5**).** Compound **1** (95 mg, 0.09 mmol) was dissolved in 15 mL of THF and cooled to –78 °C. To this solution was added 1.7 mL (0.25 mmol) of a freshly prepared solution of LiC(CH<sub>3</sub>)<sub>2</sub>CN in THF. The resulting orange-brown solution was stirred for 15 min, warmed to room temperature, and then stirred for an additional 15 min. The solution was again cooled to –78 °C, and 15 μL of trifluoroacetic acid was added dropwise. The solution was then warmed to room temperature, rotary evaporated to dryness, taken up in CH<sub>2</sub>Cl<sub>2</sub>, filtered, and then purified by preparative TLC using 40:60 CH<sub>2</sub>Cl<sub>2</sub>/hexane as eluent. One major band was isolated in addition to minor amounts of **1** and two other unidentified minor yellow bands, which yielded 59 mg (58%) of **5**.

**Spectroscopic and Analytical Data for 5.** Anal. Calcd for C<sub>26</sub>H<sub>16</sub>N<sub>2</sub>O<sub>9</sub>Os: C, 29.15; H, 1.51; N, 2.61. Found: C, 28.91; H, 2.21; N, 2.38. IR (ν CO) in hexane: 2077(m), 2047(s), 2023(s), 1992(br), 1975(w), 1060(w), 1944(w). <sup>1</sup>H NMR in CDCl<sub>3</sub>: 8.89 (m, H(2)), 8.08 (s, H(9)), 8.04 (d, H(5)), 7.90 (dd, H(7)), 7.84 (d, H(8)), 7.59 (dd, H(6)), 3.91 (dd, H(4)), 3.18 (M, 2H, H(3), H(3)<sup>1</sup>), 1.38 (s, CH<sub>3</sub>), 1.24 (s, CH<sub>3</sub>), –14.20 (s, hydride).

**Synthesis of Os<sub>3</sub>(CO)<sub>9</sub>(μ<sub>3</sub>-η<sup>2</sup>-C<sub>13</sub>H<sub>9</sub>(9-*n*-Bu)N)(μ-H)<sub>2</sub>(**6**) and Os<sub>3</sub>(CO)<sub>9</sub>(μ<sub>3</sub>-η<sup>2</sup>-C<sub>13</sub>H<sub>9</sub>(5- or 6-*n*-Bu)N)(μ-H) (**7** and **8**).** Compound **1** (105 mg, 0.10 mmol) was dissolved in 10 mL of THF and cooled to –78 °C. Li<sup>n</sup>Bu (220 μL of 1.45 M in hexane, 0.32 mmol) was slowly added to the solution with stirring. After stirring for 1 h at –78 °C and 1 h at 0 °C, 25 μL of trifluoroacetic acid (0.32 mL) was slowly added with stirring, and then the reaction mixture was rotary evaporated, taken up in CH<sub>2</sub>Cl<sub>2</sub>, filtered, and separated by preparative TLC with 30:70 CH<sub>2</sub>Cl<sub>2</sub>/hexane to yield three product bands in addition to a small amount of unreacted **1**. A fast moving yellow band,

23 mg of **6** (23%), and two green bands, 23 mg of **7** (23%) and 22 mg of **8** (22%), were isolated and identified.

**Spectroscopic and Analytical Data for 6.** Anal. Calcd for C<sub>26</sub>H<sub>19</sub>NO<sub>9</sub>Os<sub>3</sub>: C, 29.46; H, 1.81; N, 1.32. Found: C, 29.66; H, 1.98; N, 1.52. IR (ν CO) in hexane: 2096(m), 2072(s), 2049(s), 2010(s), 1998(s), 1976(m), 1969(w) cm<sup>-1</sup>. <sup>1</sup>H NMR in CDCl<sub>3</sub>: δ 8.17 (d, H(2)), 7.86 (d, H(4)), 7.50 (d, H(8)), 7.27 (m, 2H, H(6) and H(7)), 7.03 (d, H(5)), 6.56 (dd, H(3)), 2.73 (dd, H(9)), 1.48 (m, 1H), 1.20–0.72 (m, 5H), 0.67 (t, CH<sub>3</sub>), –14.30 (d, <sup>2</sup>J<sup>1</sup>H–<sup>1</sup>H = 1.2 Hz, hydride), –15.04 (d, <sup>2</sup>J<sup>1</sup>H–<sup>1</sup>H = 1.2 Hz, hydride).

**Spectroscopic and Analytical Data for 7.** Anal. Calcd for C<sub>26</sub>H<sub>17</sub>NO<sub>9</sub>Os<sub>3</sub>: C, 29.52; H, 1.62; N, 1.32. Found: C, 29.78; H, 2.00; N, 1.24. IR (ν CO) in hexane: 2111(w), 2076(m), 2049(s), 2025(s), 1997(m), 1976(w) cm<sup>-1</sup>. <sup>1</sup>H NMR in CDCl<sub>3</sub>: δ 9.06 (d, H(2)), 8.71(d, H(4)), 8.11 (s, H(5)), 7.91 (d, H(8)), 7.91 (s, H(9)), 7.56 (d, H(7)), 7.17 (dd, H(3)), 2.81 (dd, 2H), 1.70 (m, 2H), 1.41 (m, 2H), 0.94 (t, CH<sub>3</sub>), –13.55 (s, hydride).

**Spectroscopic and Analytical Data for 8.** Anal. Calcd for C<sub>26</sub>H<sub>17</sub>NO<sub>9</sub>Os<sub>3</sub>: C, 29.52; H, 1.62; N, 1.32. Found: C, 29.77; H, 1.76; N, 1.32. IR (ν CO) in hexane: 2096(m), 2077(m), 2050(s), 2026(s), 1997(m), 1976(w) cm<sup>-1</sup>. <sup>1</sup>H NMR in CDCl<sub>3</sub>: δ 9.12 (d, H(2)), 8.75 (d, H(4)), 8.68 (s, H(5)), 8.25 (d, H(8)), 7.93 (dd, H(7)), 7.57 (d, H(6)), 7.21 (dd, H(3)), 3.07 (t, 2H), 1.70 (m, 2H), 1.49 (m, 2H), 0.97 (t, CH<sub>3</sub>), –12.97 (s, hydride).

**X-ray Structure Determination of 3 and 7.** Crystals of each compound for X-ray examination were obtained from saturated solutions in hexane/dichloromethane solvent systems at –20 °C. Suitable crystals of each were mounted on glass fibers, placed in a goniometer head on the diffractometer, and centered optically. For **3**, unit cell parameters and an orientation matrix for data collection were obtained by using the centering program in the CAD4 system; crystals of **7** were all too small for the CAD4, so data were collected on the Bruker SMART CCD system at the Center for Molecular Structure (CMoS) at California State University Fullerton. Details of the crystal data for each compound are given in Table 1. For **3**, the actual scan range was calculated by scan width – scan range + 0.35 tan θ, and backgrounds were measured by using the moving-crystal moving-counter technique at the beginning and end of each scan. Two representative reflections were monitored every 2 h as a check on instrument and crystal stability. For **7**, frames were collected using the SMART8 software, and the data were processed with the program SAINT9 at CMoS. Lorentz, polarization, and decay corrections were applied to each set of raw crystal data, and the data for **7** were also corrected for absorption using SADABS.<sup>10</sup> The weighting scheme used during refinement for **7** was 1/σ<sup>2</sup>, based on counting statistics; for **3**, an adjusted weighting scheme in SHELXL was employed. Each of the structures was solved by the Patterson method using SHELXTL/PC,<sup>11</sup> which revealed the positions of the osmium atoms. Remaining non-hydrogen atoms were found by successive refinement and ΔF syntheses. The hydrides bridging the Os(1) and Os(3) atoms in each molecule were positioned using HYDEX,<sup>12</sup> and other hydrogen atoms were placed in their expected chemical positions using the HFIX command in SHELXTL/PC and were included as riding atoms. All non-hydrogen atoms were refined anisotropically in **7**, but in **3**, the crystal was very small and of poor diffraction quality, so the carbon, oxygen, and nitrogen atoms were given separate, group isotropic temperature factors, which were refined, and in addition, general restraints to carbonyl and ring atom distances were added in order to refine the structure. Data processing for **3** was carried out on PC's using SCAD4.<sup>13</sup>

(8) SMART V4.210; Bruker AXS: Madison, WI 53719, 1996.

(9) SAINT V4.05; Bruker AXS: Madison, WI 53719, 1996.

(10) Sheldrick, G. SADABS; University of Goettingen, Germany, 1996.

(11) SHELXTL/PC, V5.03; Bruker AXS: Madison, WI 53719, 1997.

(12) Orpen, A. G. J. *J. Chem. Soc., Dalton Trans.* **1980**, 2509.



Neutral atom scattering factors and values of  $\Delta f'$  and  $\Delta f''$  were from Volume C of the International Tables for Crystallography.<sup>14</sup> For both crystals, structure solution, refinement, and preparation of figures and tables for publication were carried out on PC's by using SHELXTL-PC.<sup>10</sup>

---

(13) SCAD4; Bruker AXS: Madison, WI 35719.

(14) *International Tables for X-ray Crystallography, Vol. C*; Kluwer Academic Publishers: Dordrecht, 1992; Tables 6.1.1.4, pp 500–502, and 4.2.6.8, pp 219–222.

**Acknowledgment.** We gratefully acknowledge the support of the National Science Foundation (CHE96 25367) for support of this research.

**Supporting Information Available:** Complete distances and bond angles, atomic coordinates, anisotropic thermal parameters, and hydrogen coordinates for **3** and **7**, Tables 4–11. This material is available free of charge via the Internet at <http://pubs.acs.org>.

OM9902535